Improved Performance of Optical F-OFDM over Conventional OFDM for Residual Frequency Offset Compensation

Jian Zhao

Photonic Systems Group, Tyndall National Institute and University College Cork, Lee Maltings, Dyke Parade, Cork, Ireland (Email: jian.zhao@tyndall.ie)

Abstract We experimentally show that the tolerance of residual frequency offset (RFO) to subcarrier spacing ratio of optical fast OFDM is four times greater than that of conventional OFDM, when multi-tap equalizers are applied for the RFO compensation.

Introduction

Optical fast orthogonal frequency division multiplexing (F-OFDM)[1-6], with a subcarrier spacing equal to half of that in the conventional OFDM, is a promising multicarrier scheme. The subcarrier multiplexing/demultiplexing can be implemented using a discrete cosine transform (DCT) pair. Because the properties of the DCT differ from those of the discrete Fourier transform (DFT), a guard interval (GI) designed specifically for optical F-OFDM was proposed[2]. It is shown that by using a symmetric extension (SE) rather than cyclic extension based GI, the F-OFDM subcarriers can be demultiplexed by DCT without inter-carrier interference (ICI) and the chromatic dispersion (CD) can be compensated with one-tap equalizers.

However, carrier frequency offset due to the frequency mismatch between the transmitter laser and local oscillator would introduce ICI[7-8]. An algorithm is commonly used at the training stage to estimate the frequency offset. However, as the laser wavelengths drift over time, residual frequency offset (RFO) always exists. Clearly, larger tolerance against the RFO not only relaxes the specification of frequency offset estimation algorithm but also enhances the robustness against laser wavelength instability.

Recently, we showed that multi-tap equalizers could greatly mitigate RFO-induced ICI in optical F-OFDM[3]. However, only theoretical study was presented and no experimental verification was reported. In this paper, we experimentally investigate the performance of multi-tap equalizers in RFO compensation. We compare optical F-OFDM with conventional OFDM using 16 quadrature amplitude modulation (16QAM), and show that F-OFDM exhibits greatly improved performance over the conventional OFDM when multi-tap equalizers are applied for the RFO compensation. This advantage, together with fast channel estimation and compensation scheme[5], makes optical F-OFDM a promising technique for the future optical packet networks using fast tunable transceivers.

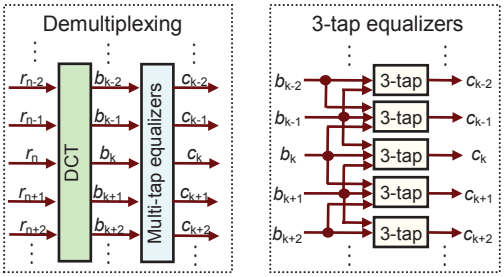

Fig. 1. Configuration of demultiplexing and an example of three-tap equalizers for the RFO-induced ICI compensation.

Principle

Fig. 1 depicts the demultiplexing and three-tap equalizers in an F-OFDM system. Assuming the subcarrier data of an OFDM (F-OFDM) symbol are a_k, k = 0 … N-1, where N is the subcarrier number. The decoded data in OFDM, b_k, are:

$$b_k = a_k * DFT\{\exp(j \cdot 2\pi f_{RFO} \cdot T \cdot n), n = 0 \ldots N-1\} = a_k * h_k \quad (1)$$

where f_{RFO} and T are the RFO and the time interval between samples, respectively, where * represents the convolution. h_0 and $h_{k,\,k\neq 0}$, are the signal and the ICI coefficients, respectively. The subcarrier spacing f_s is equal to $1/(NT)$. On the other hand, the decoded subcarrier data b_k in optical F-OFDM are:

$$b_k = a_k * DFT\{H_n, n = 0 \ldots 2N_F - 1\} = a_k * h_k \quad (2)$$

where H_n = [exp(j·2πf_{RFO}·T·0)…exp(j·2πf_{RFO}·T·(N_F-1)), exp(j·2πf_{RFO}·T·(N_F-1))…exp(j·2πf_{RFO}·T·0)]. In (2), N_F represents the F-OFDM subcarrier number, and the subcarrier spacing f_s is equal to $1/(2N_FT)$. We compare F-OFDM with conventional OFDM in two scenarios: 1) the same RFO to subcarrier spacing ratio; 2) the same processed DFT or DCT point size (N = N_F). In each scenario, f_{RFO} and T are kept the same for these two schemes. Consequently, scenario 1 can be obtained by setting N = 2N_F. The first scenario is a fair comparison from the scientific perspective whilst the second one is used for comparison in practical implementation.

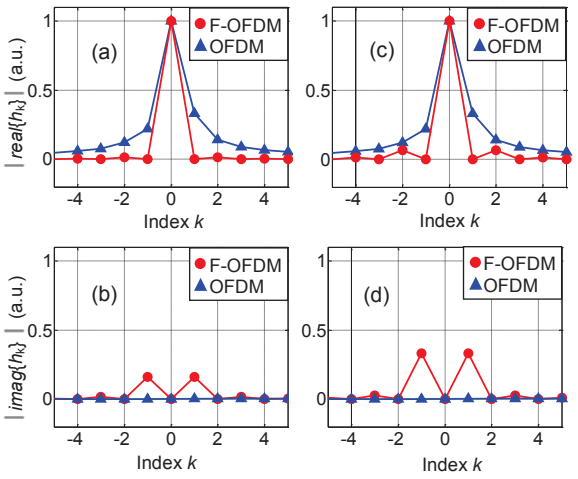

Fig. 2. $|real\{h_k\}|$ ((a)&(c)) and $|imag\{h_k\}|$ ((b)&(d)). (a)&(b): scenario 1, $N = 2N_F = 256$, f_{RFO} and f_s are 12 and 46.8 MHz, respectively; (c)&(d): scenario 2, $N = N_F = 256$, f_{RFO} is 12 MHz, and f_s is 46.8 and 23.4 MHz for conventional OFDM and F-OFDM, respectively.

Fig. 2 depicts the absolute amplitude of real and imaginary parts of h_k. Fig. 2(a) shows that in scenario 1, $|real\{h_k\}|$ in F-OFDM (circles) are almost zero for $k \neq 0$ whilst those in conventional OFDM (triangles) have much higher values. The ICI in optical F-OFDM is dominated by $imag\{h_{-1}\}$ and $imag\{h_1\}$ as shown in Fig. 2(b). This implies that the ICI on the k^{th} subcarrier is mainly from the adjacent $(k\text{-}1)^{th}$ and $(k\text{+}1)^{th}$ subcarriers. In scenario 2, the subcarrier spacing of F-OFDM is reduced to 23.4 MHz. Consequently, at a fixed f_{RFO}, the values of the ICI coefficients in optical F-OFDM increase when compared to Fig. 2(a)&(b). However, $|real\{h_k\}|$ still have much lower values than those in conventional OFDM for $k \neq 0$, and most of the ICI power remains in $imag\{h_{-1}\}$ and $imag\{h_1\}$.

Experimental setup

Fig. 3 shows the experimental setup. Two bipolar four amplitude-shift-keying (4ASK) data were encoded with gray coding. In scenario 1, the IDCT used 128 points, of which 102 subcarriers were used for data modulation and 20 subcarriers were zero-padded to avoid aliasing. The first six subcarriers were not modulated to allow for AC-coupled amplifiers and insertion of pilot tones for phase estimation. In scenario 2, the numbers of data and zero-padded subcarriers were doubled with IDCT point size of 256. After IDCT and parallel-to-serial (P/S) conversion, 6 samples were added as an SE-based GI. The generated F-OFDM signal was downloaded to a 12-GS/s arbitrary waveform generator. The subcarrier spacing was 46.8 and 23.4 MHz for scenarios 1 and 2, respectively.

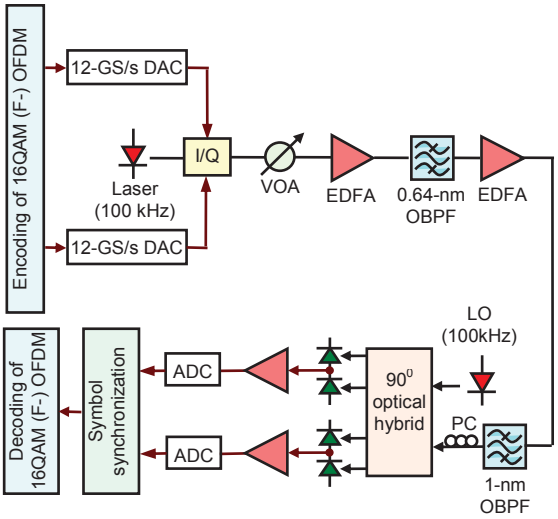

Fig. 3. Experimental setup

A laser with 100-kHz linewidth was used to generate the optical carrier. The F-OFDM signal was fed into an optical I/Q modulator with a peak-to-peak driving swing of $0.5V_\pi$. At the receiver, the optical signal was detected with a pre-amplified coherent receiver and a variable optical attenuator (VOA) was used to vary the optical signal-to-noise ratio (OSNR) for the bit error rate (BER) measurements. The pre-amplifier was followed by an optical band-pass filter (OBPF) with a 3-dB bandwidth of 0.64 nm, a second EDFA, and another OBPF with a 3-dB bandwidth of 1 nm. A polarization controller (PC) was used to align the polarization of the filtered signal before entering the signal path of a 90^0 optical hybrid. The optical outputs of the hybrid were connected to two balanced photodiodes with 40-GHz 3-dB bandwidths, amplified by 40-GHz electrical amplifiers, and captured using a 50-GS/s real-time oscilloscope. The precise RFO values were controlled in the digital domain at the receiver for investigation. The receiver algorithms included interpolation, symbol synchronization, phase estimation, and equalization (Fig. 1). For comparison, the conventional OFDM was also implemented with the FFT point size of 256. The total number of measured 16QAM symbols was 240,000.

Results and discussions

Fig. 4(a) shows BER versus received OSNR, and (b)-(e) show the recovered constellation diagrams. When f_{RFO} = 5 MHz, the RFO-induced ICI was not severe. Therefore the performance was similar for all three cases, and the required OSNR to achieve a BER of 1×10^{-3} was ~15 dB. When the RFO was increased to 15 MHz, the performance of conventional OFDM was degraded significantly even using seven-tap equalizers. In contrast, for F-OFDM using 128

subcarriers (f_s = 46.8 MHz), the performance was still similar to that at 5-MHz RFO. In scenario 2, as the subcarrier spacing of F-OFDM was reduced to 23.4 MHz, a performance penalty was observed. However, a BER lower than 2×10^{-3} could still be achieved at 18.5-dB OSNR, which confirmed the performance advantage of optical F-OFDM over conventional OFDM in the RFO compensation.

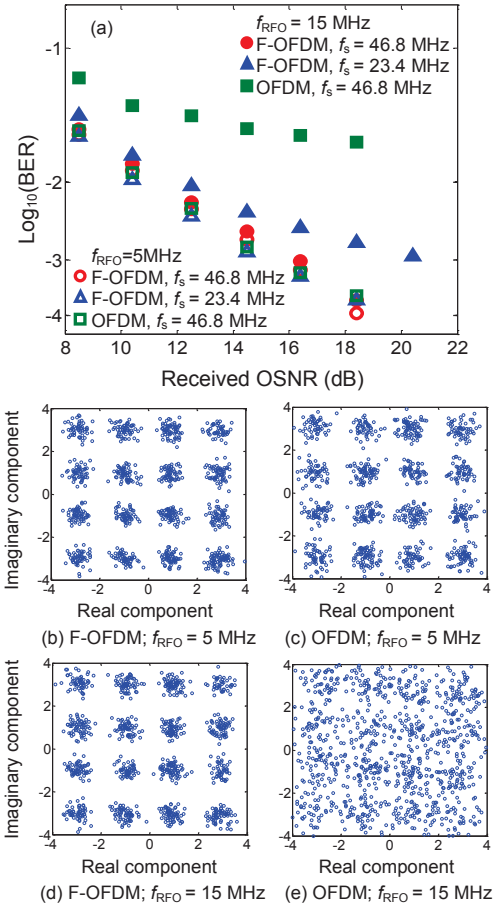

Fig. 4. (a) BER versus received OSNR using seven-tap FIR equalizers. (b)-(e): recovered constellation diagrams for f_{RFO} of 5 and 15 MHz at 18.5-dB OSNR and 46.8-MHz f_s.

Fig. 5 shows BER versus the RFO. It can be clearly seen that the BER of conventional OFDM increased quickly as the RFO increased. On the other hand, F-OFDM exhibited a RFO tolerance range four and two times greater than that of the conventional OFDM in scenarios 1 and 2 respectively. Fig. 6 illustrates BER versus RFO for F-OFDM using multi-tap equalizer with different tap numbers. As expected (see Fig. 2), a three-tap equalizer could compensate most of the ICI, resulting in significant performance improvement over a one-tap equalizer. Increasing the tap number to five could further improve the performance. As h_k is nearly zero for $|k|>2$ (see Fig. 2), performance became stable for seven-tap equalizers.

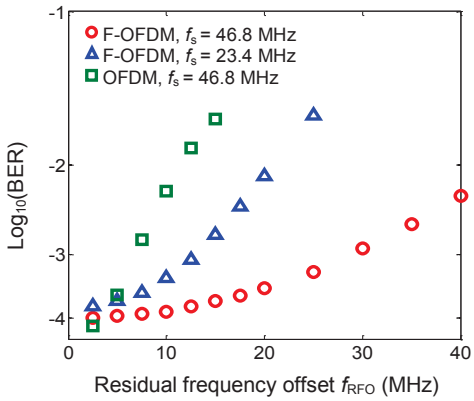

Fig. 5. BER versus f_{RFO} at 18.5-dB OSNR using seven-tap FIR equalizers.

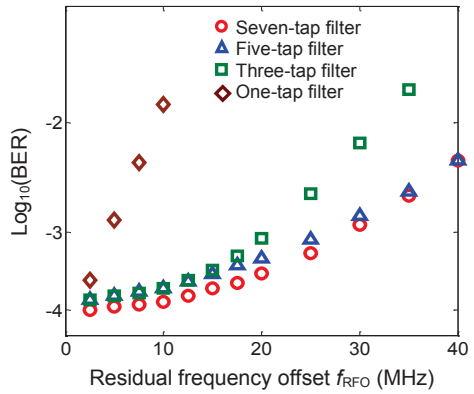

Fig. 6. BER versus f_{RFO} for F-OFDM using different tap numbers at 18.5-dB OSNR and 46.8-MHz f_s.

Conclusions

We have experimentally demonstrated the performance advantage of 16QAM optical F-OFDM over 16QAM conventional OFDM when multi-tap equalizers are applied for the RFO compensation. The results show that the tolerance of RFO to subcarrier spacing ratio of F-OFDM is four times greater than that of the conventional OFDM. This makes optical F-OFDM a promising technique for optical packet networks using fast tunable transceivers.

Acknowledgements

This work was supported by Science Foundation Ireland under grant number 11/SIRG/I2124 and 06/IN/I969, and the EU 7th Framework Program under grant agreement 318415 (FOX-C).

References

[1] S.K.Ibrahim et al, ECOC'10, PDP3.4.
[2] J.Zhao et al, PTL **24**, 34 (2012).
[3] J.Zhao et al, PTL **24**, 2284 (2012).
[4] E.Giacoumidis et al, PTL **24**, 52 (2012).
[5] J.Zhao et al, Opt. Express **21**, 2500 (2013).
[6] C.Lei et al, Opt. Express **19**, 15275 (2011).
[7] T.M.Schmidl et al, IEEE Trans. Commun. **45**, 1613 (1997).
[8] F.Buchali et al, ECOC'08, Mo.4.D.4.